



GENETICS

The PCNA–Pol δ complex couples lagging strand DNA synthesis to parental histone transfer for epigenetic inheritance

Albert Serra-Cardona^{1†}, Xu Hua^{1†}, Seth W. McNutt², Hui Zhou¹, Takenori Toda³, Songtao Jia³, Feixia Chu², Zhiguo Zhang^{1*}

Inheritance of epigenetic information is critical for maintaining cell identity. The transfer of parental histone H3-H4 tetramers, the primary carrier of epigenetic modifications on histone proteins, represents a crucial yet poorly understood step in the inheritance of epigenetic information. Here, we show the lagging strand DNA polymerase, Pol δ , interacts directly with H3-H4 and that the interaction between Pol δ and the sliding clamp PCNA regulates parental histone transfer to lagging strands, most likely independent of their roles in DNA synthesis. When combined, mutations at Pol δ and Mcm2 that compromise parental histone transfer result in a greater reduction in nucleosome occupancy at nascent chromatin than mutations in either alone. Last, PCNA contributes to nucleosome positioning on nascent chromatin. On the basis of these results, we suggest that the PCNA–Pol δ complex couples lagging strand DNA synthesis to parental H3-H4 transfer, facilitating epigenetic inheritance.

INTRODUCTION

Inheritance of epigenetic information encoded by chromatin plays a critical role in the maintenance of gene expression states and cell identity in multicellular organisms (1, 2). The basic repeating unit of chromatin is the nucleosome, composed of 147 bp of DNA wrapped around a histone octamer containing one (H3-H4)₂ tetramer and two histone H2A-H2B dimers (3). Unique posttranslational modifications on histone proteins organize chromatin into different domains including euchromatin and heterochromatin. During mitotic cell division, both the positioning of nucleosomes along DNA and specific histone modifications in each chromatin domain can be transmitted into two daughter cells for the inheritance of cell identity. Misregulation in this process is linked to many human diseases including cancer (4). However, how this fundamental cellular process is achieved remains elusive.

DNA replication–coupled nucleosome assembly is the initial step in the inheritance of epigenetic information (5–7). Nucleosomes ahead of DNA replication forks are transiently disassembled to allow the DNA replication machinery to replicate DNA. Immediately following DNA replication, parental histones H3-H4 tetramers are transferred to either the leading or lagging strand of the DNA replication fork for nucleosome formation. In the meantime, newly synthesized H3-H4 tetramers, which have distinct modifications from parental H3-H4, are also deposited to the replicating DNA strands for nucleosome formation to accommodate the duplication of DNA such that parental and newly synthesized H3-H4 tetramers form distinct nucleosomes on nascent chromatin (8). Subsequently, a read-write mechanism helps restore some histone modifications: The enzyme responsible for a particular modification first binds to nucleosomes formed with parental H3-H4 carrying the modification

and then modifies neighboring nucleosomes formed with new H3-H4 tetramers (9–13). Recently, it has been shown that parental H3-H4 tetramers, when transferred to either leading or lagging strands of DNA replication forks, can remember their positions along the DNA (14, 15), possibly through the aid of chromatin remodelers. Therefore, the transfer of parental histone H3-H4 tetramers is a key step in the inheritance of epigenetic information. However, it remains largely unknown how this process is regulated. Furthermore, it is largely unexplored how two nucleosome assembly pathways, parental histone transfer and deposition of new H3-H4, are coordinated for the inheritance of epigenetic information.

Chromatin assembly factor 1 (CAF-1) is the primary histone chaperone that deposits newly synthesized H3-H4 onto replicating DNA for nucleosome assembly (16–20). Recent studies have shown that CAF-1 facilitates right-handed DNA wrapping of H3-H4 tetramer, a conformation in contrast to the left-handed DNA wrapping in the nucleosome (21). Furthermore, CAF-1 interacts with proliferating cell nuclear antigen (PCNA) (17, 22), and this interaction is important for CAF-1 to deposit newly synthesized H3-H4 onto replicating DNA. PCNA is essential for DNA replication and DNA repair and interacts with many proteins in these processes (23). Last, PCNA's role in regulating nucleosome assembly of newly synthesized H3-H4 is conserved from yeast to human cells (16–19).

We and others have discovered two conserved pathways mediating the transfer of parental histones onto the leading and lagging strands of DNA replication forks (24–27). Specifically, yeast Dpb3 and Dpb4 (POLE3 and POLE4 in mammalian cells), the non-essential subunits of leading strand DNA polymerase ϵ , interact with H3-H4 and promote the transfer of parental (H3-H4)₂ to the leading strands (24, 26). On the other hand, minichromosome maintenance complex component 2 (Mcm2), a member of the minichromosome maintenance complex (MCM) helicase, participates in the transfer of parental (H3-H4)₂ to the lagging strands along with the adaptor protein chromosome transmission fidelity (Ctf) 4 and DNA polymerase α (25–27). However, our understanding of this critically important process is far from complete. For instance, Mcm2 is far removed from Okazaki fragments synthesized on lagging

¹Institute for Cancer Genetics, Department of Pediatrics and Department of Genetics and Development, Columbia University Irving Medical Center, New York, NY 10019, USA. ²Department of Molecular, Cellular, and Biomedical Sciences, University of New Hampshire, Durham, NH 03824, USA. ³Department of Biological Sciences, Columbia University, New York, NY 10027, USA.

*Corresponding author. Email: zz2401@cumc.columbia.edu

†These authors contributed equally to this work.

strand. Furthermore, after Pol α synthesizes a RNA-DNA primer to initiate synthesis of a Okazaki fragment, PCNA-DNA polymerase (Pol δ) replaces Pol α and uses the RNA-DNA primer to continue DNA synthesis of the Okazaki fragment followed by strand displacement synthesis for the generation of 5'-RNA flap of the proceeding Okazaki fragment and the removal of this flapped RNA primer by flap structure-specific endonuclease 1 (Fen1) and DNA replication helicase/nuclease 2 (Dna2) nucleases and subsequent ligation of these two Okazaki fragments (28). Replacement of Pol α by Pol δ for Okazaki fragment synthesis suggests that other factors following Pol α may help deposit parental H3-H4 on lagging strands. Furthermore, these repeated cycles of primer synthesis by Pol α , Okazaki fragment synthesis by Pol δ , and processing and maturation of Okazaki fragments on lagging strand make it challenging to envision how parental (H3-H4)₂ tetramers are deposited on Okazaki fragments to remember their positions along the DNA.

Here, we show that PCNA is also important for parental histone transfer in budding yeast. Furthermore, the mutant allele of PCNA (*pol30-79*) that affects parental histone transfer is different from the mutant allele of PCNA (*pol30-8*) that impairs CAF-1-mediated nucleosome assembly of newly synthesized H3-H4. We also show that PCNA regulates parental histone transfer, most likely through its interaction with DNA Pol δ . Last, we report that PCNA also contributes to nucleosome positioning at nascent chromatin. On the basis of these studies, we propose that the PCNA-Pol δ complex couples lagging strand DNA synthesis to parental histone transfer.

RESULTS

The *pol30-79*, but not *pol30-8* and *pol30-6*, mutant allele affects parental histone transfer

We have shown previously that three site-specific mutants of PCNA (called *pol30-8*, *pol30-79* and *pol30-6* as PCNA is encoded by the *POL30* gene in *Saccharomyces cerevisiae*) affect heterochromatin silencing in budding yeast (19). While the *pol30-8* mutant allele reduces heterochromatin silencing through its impact on the interaction between PCNA and CAF-1, a histone chaperone involved in deposition of newly synthesized H3-H4 onto replicating DNA, genetic evidence suggests that *pol30-79* and *pol30-6* mutants reduce heterochromatin silencing through a mechanism independent of CAF-1 (19). As mutations defective in parental histone transfer discovered so far also show a defect in heterochromatin silencing in yeast and in mouse embryonic stem (ES) cells (24–26), we analyzed the impact of each of these three alleles (Fig. 1A) on the distribution of histone trimethylation of histone H3 lysine 4 (H3K4me3) and acetylation of histone H3 lysine 56 (H3K56ac), which are surrogate marks on parental and newly synthesized H3, respectively, between the leading and lagging DNA strands using eSPAN (enrichment and sequencing of protein-associated nascent DNA) (24, 29). Briefly, to perform H3K4me3 and H3K56ac eSPAN, yeast cells arrested at G₁ using alpha-factor were released into early S phase in the presence of nucleotide analog 5-bromo-2'-deoxyuridine (BrdU), which is incorporated into newly synthesized DNA. Chromatin was then digested with micrococcal nuclease (MNase), which cleaves DNA between nucleosomes. A small fraction of the processed chromatin was collected for library preparation as the input sample and for analyzing DNA synthesis by using BrdU immunoprecipitation followed by strand-specific sequencing (MNase BrdU-IP-ssSeq). The rest of chromatin samples was immunoprecipitated with

antibodies against H3K56ac or H3K4me3 [chromatin immunoprecipitation (ChIP)]. The ChIP DNA was then denatured into single-stranded DNA for BrdU immunoprecipitation to enrich H3K56ac- and H3K4me3-associated nascent DNA and subsequent strand-specific sequencing (eSPAN) (Fig. 1B). To analyze the eSPAN results, the eSPAN bias, which measures the relative amount of H3K4me3 and H3K56ac at the leading and lagging strands, was calculated by comparing sequencing reads of Watson and Crick strands at each origin. Furthermore, to mitigate the potential contributions to the H3K56ac and H3K4me3 eSPAN bias from the defects in DNA synthesis, we normalized the eSPAN reads against BrdU-IP-ssSeq reads. If H3K56ac and H3K4me3 are equally distributed to leading and lagging strands, then H3K56ac and H3K4me3 eSPAN bias would be close to zero (Fig. 1B). H3K4me3 and H3K56ac eSPAN signals in *pol30-6* and *pol30-8* mutant strains showed a relatively similar distribution between the leading and lagging strands based on the inspection of sequence reads at individual origins such as *ARS508*, as well as analysis of eSPAN bias at each of the 20 individual nucleosomes surrounding each of 134 early replication origins (fig. S1, A to D), indicating that like wild-type (WT) cells, H3K4me3 and H3K56ac are almost equally distributed to leading and lagging strands of DNA replication forks in these two PCNA mutant cells. On the other hand, H3K4me3 and H3K56ac eSPAN peaks in *pol30-79* mutant cells displayed a leading- and lagging-strand bias, respectively, based on the inspection of the eSPAN signals at individual origins such as *ARS508* (Fig. 1C) as well as on the analysis of eSPAN bias at each of 20 individual nucleosomes at each of 134 early replication origins (Fig. 1, D and E), indicating that parental H3-H4 and newly synthesized H3-H4 are enriched at leading and lagging strands, respectively, in *pol30-79* mutant cells. We also analyzed the average bias ratio of each of the 20 nucleosomes around 134 early replication origins in these three mutant cells (Fig. 1, F and G). Both *pol30-6* and *pol30-8* showed a very small bias ratio for H3K4me3 and H3K56ac eSPAN, similar to the WT strain. In contrast, H3K4me3 and H3K56ac eSPAN signals in *pol30-79* displayed a consistent leading and lagging bias, respectively. This bias pattern is similar to what we observed in mutations at the histone-binding domains of Mcm2 and Pol1 (the catalytic subunit of Pol α primase) that compromise the histone transfer to lagging strands (25). Together, these results indicate that the *pol30-79* mutation, but not *pol30-6* and *pol30-8* mutations, impairs the transmission of parental H3-H4 to lagging strands during DNA replication.

The effects of *pol30-79* mutation on parental histone transfer are unlikely due to its impact on DNA synthesis

The two residues mutated in *pol30-79* are at the interdomain connecting loop where almost all of PCNA's known partners could bind, including DNA polymerases ϵ and δ (23). Therefore, it would be possible that the compromised parental H3-H4 segregation to lagging strands observed in *pol30-79* was due to a defect in lagging strand synthesis. Arguing against this idea, we observed that defects in DNA synthesis detected by BrdU-IP-ssSeq, which was generated for the normalization of H3K56ac and H3K4me3 eSPAN results in Fig. 1, in *pol30-79* cells, while larger than WT cells, were slightly less pronounced than in *pol30-6* mutant cells (fig. S2A). This result is consistent with previously published studies indicating that the *pol30-6* mutation compromises DNA synthesis more markedly than *pol30-79* mutation in vitro and that *pol30-6* mutant cells were more

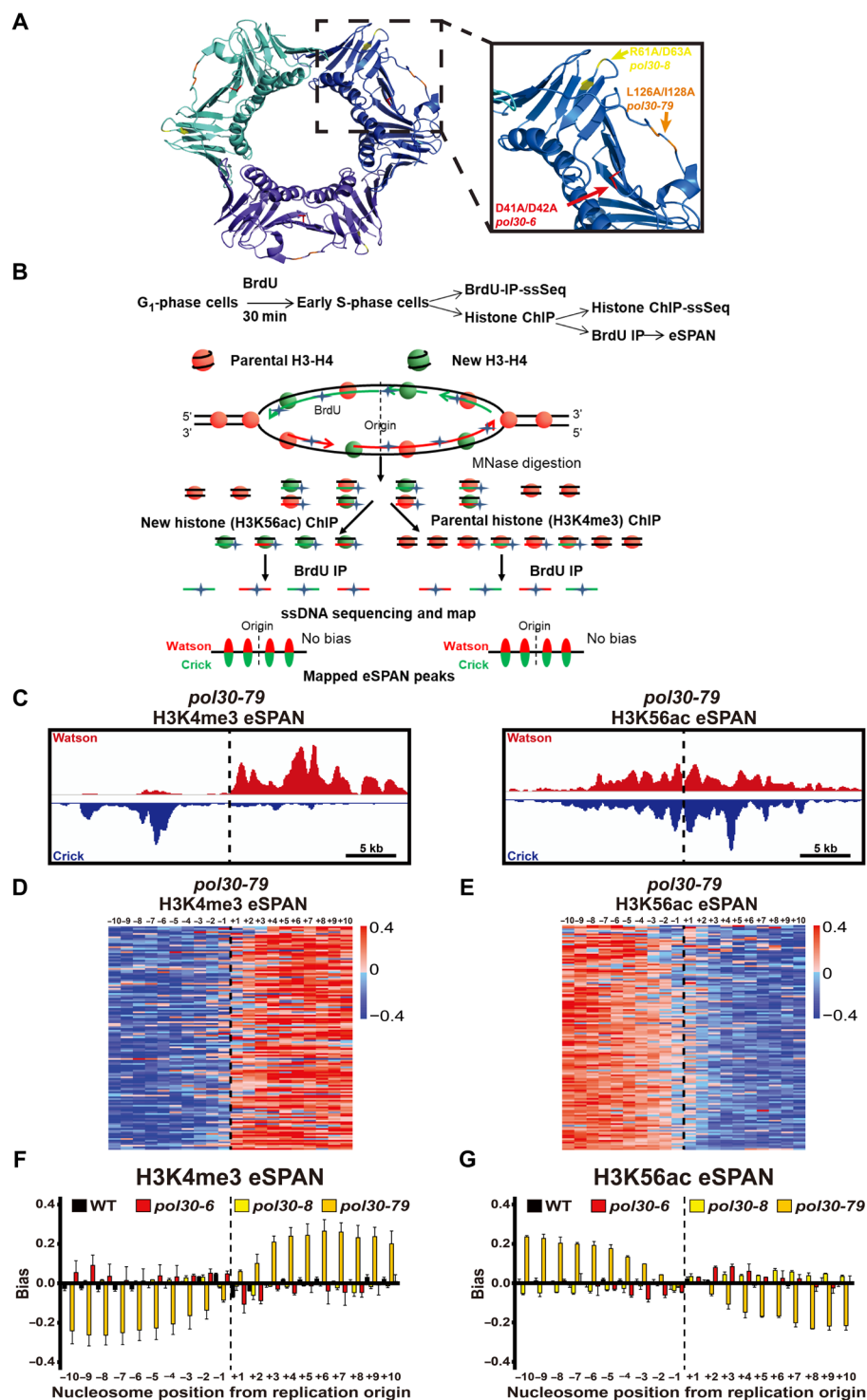


Fig. 1. The *pol30-79*, but not *pol30-6* and *pol30-8* mutations, reduces the transfer of parental histone transfer to lagging strands during DNA replication. (A) Representation of the PCNA homotrimer structure and the location of residues mutated in *pol30-6*, *pol30-8*, and *pol30-79* (Protein Data Bank entry 2OD8.pdb). Each monomer is represented in a different color. (B) An experimental outline of eSPAN procedures. In this hypothetical model, both parental and new H3-H4 are equally distributed to leading and lagging strands of DNA replication forks. Therefore, eSPAN bias is close to zero. ssDNA, single-stranded DNA. (C) Snapshots of H3K4me3 (left) and H3K56ac (right) eSPAN read density around early replication origin *ARS508* in *pol30-79* cells. Red and blue represent eSPAN sequence reads at Watson and Crick strands, respectively. (D and E) Heatmap of H3K4me3 (D) and H3K56ac (E) eSPAN bias at each of the 20 individual nucleosomes around each of 134 early replication origins in *pol30-79* cells. The average of two biological replicates is presented. The eSPAN bias at each of the 20 nucleosomes surrounding each of 134 early replication origins was calculated using the formula: $(W - C)/(W + C)$. *W* and *C*, sequence read of Watson and Crick strand at each nucleosome, respectively. (F and G) The average H3K4me3 (F) and H3K56ac (G) eSPAN bias at each of 20 individual nucleosomes of 134 early replication origins in WT and three PCNA mutant cells. The average of two biological replicates is represented as mean + SEM.

sensitive to DNA damage agents than *pol30-79* cells (30, 31). Together, these results argue that a defect in DNA synthesis may not directly impair parental histone transfer to lagging strands.

Because BrdU-IP-ssSeq results in fig. S2A were generated using chromatin sheared by MNase digestion, the large leading strand bias of BrdU-IP-ssSeq in *pol30-79* cells compared to WT cells could be due to either defects in nucleosome assembly and/or DNA synthesis. Therefore, to measure the potential effects of *pol30-79* mutation on nucleosome assembly alone, we compared the bias of BrdU-IP-ssSeq using DNA fragmented by sonication (sonication-BrdU-IP-ssSeq) to that of BrdU-IP-ssSeq using chromatin digested with MNase (MNase-BrdU-IP-ssSeq). In this way, sonication-BrdU-IP-ssSeq allows us to monitor the impact of the *pol30-79* mutation on DNA synthesis without the complications from defects in nucleosome assembly. As shown in Fig. 2 (A, C, and E), in WT cells, sonication- and MNase-BrdU-IP-ssSeq displayed a small leading strand bias, indicating that the synthesis of the leading strand is slightly ahead of the lagging strand. Furthermore, the bias of sonication-BrdU-IP-ssSeq was similar to that of MNase-BrdU-IP-ssSeq, consistent with the idea that DNA replication and nucleosome assembly are tightly coupled in WT cells (5, 32). In contrast, in *pol30-79* cells, the leading-strand bias of MNase-BrdU-IP-ssSeq was much larger than that of sonication-BrdU-IP-ssSeq (Fig. 2, B, D, and F), indicating that nucleosome assembly on lagging strand in *pol30-79* mutant cells is compromised, making the nascent chromatin of lagging strands in the *pol30-79* cells more susceptible to digestion by MNase. We also calculated the replication-intermediate (ReIN) score, which normalizes the MNase-BrdU-IP-ssSeq signals against the corresponding sonication-BrdU-IP-ssSeq signals to minimize the potential contribution of each mutation on DNA synthesis to nucleosome occupancy (33). As shown in Fig. 2 (G and H), we observed an almost equal nucleosome occupancy between leading and lagging strands at early replication origins in WT cells. On the other hand, nucleosome occupancy at nascent chromatin of lagging strands was much lower than that of leading strands in the *pol30-79* mutant cells (Fig. 2, I and J), likely due to defects in parental histone transfer to lagging strands. Together, these results strongly indicate that the defects in the transfer of parental H3-H4 to lagging strands in *pol30-79* are unlikely caused by a defect in DNA synthesis, but at the same time, these results cannot completely rule out this possibility.

Mutations at the PCNA binding site of two subunits of Pol δ (Pol3 and Pol32) lead to defects in parental histone transfer

PCNA interacts with proteins involved in almost all steps of Okazaki fragment processing and maturation (23). After the ligation of an Okazaki fragment with the preceding one, PCNA is unloaded by the enhanced level of genome instability (Elg1) replication factor C-like complex (29, 34). To understand how PCNA functions in parental histone transfer, we tested whether mutating any of these factors affects parental histone transfer. Deletion of the 5' flap endonuclease Fen1/Rad27, which is not essential, or depletion of the essential helicase Dna2 using the auxin-inducible degron system, did not affect the eSPAN bias of H3K4me3 and H3K56ac (fig. S2, B to I), indicating that the effects of *pol30-79* mutation on parental histone transfer are unlikely due to the reduced PCNA-Rad27 or the PCNA-Dna2 interaction. Moreover, we observed that H3K4me3 eSPAN signals in *elg1 Δ* cells showed little preference for leading or lagging strands (fig. S3, A, C, and E), suggesting that the transfer of parental histone H3-H4 to lagging strands in *elg1 Δ* cells, unlike

pol30-79 cells, is not affected to a detectable degree. H3K56ac eSPAN peaks in *elg1 Δ* exhibited a bias to lagging strands (fig. S3, B, D, and F), indicating an enrichment of newly synthesized H3K56ac on lagging strands compared to leading strands. These results are consistent with the previous study showing that retention of PCNA at lagging strands in *elg1 Δ* cells results in increased chromatin binding of CAF-1 (35), which may deposit more H3K56ac-H4 on lagging strands. Together, these results indicate that the impact of *pol30-79* mutation on parental histone transfer is most likely independent of its effect on the interaction between PCNA and each of the three proteins tested (Fen1, Dna2, and Elg1).

Next, we tested whether the PCNA–Pol δ interaction may have a role in parental histone transfer. Pol δ is composed of the catalytic subunit Pol3 and two accessory subunits, Pol31 and Pol32, with Pol3 and Pol31 being essential for cell viability. All three proteins contain a PCNA-interacting protein (PIP) motif that interacts with PCNA through the interdomain connecting loop (Fig. 3A), and all three PIP motifs are required for proper DNA synthesis as mutations at each single PIP motif have minor effects on enzymatic activities of Pol δ in vitro (36, 37). Therefore, we mutated the PIP motif of each protein and tested how each mutation affects the distribution of H3K4me3 and H3K56ac at replicating DNA strands using eSPAN. Mutating the Pol3 PIP and, to a lesser extent, the Pol32 PIP resulted in a H3K4me3 eSPAN bias toward the leading strand and a H3K56ac eSPAN bias toward the lagging strand (Fig. 3, B to G, and fig. S4). In contrast, mutating the PIP box of Pol31 had no apparent effects on the bias of H3K4me3 eSPAN or H3K56ac eSPAN signals (Fig. 3, F and G, and fig. S4). Furthermore, on the basis of sonication-BrdU-IP-ssSeq, *pol3-pip* mutation did not affect DNA synthesis to a detectable degree compared to WT cells (fig. S4E). These results indicate that mutations at the PIP box of Pol3 and Pol32, but not Pol31, affect parental histone transfer.

A separation of function *pol32* mutant affects parental histone transfer

The *POL32* gene is not essential. Therefore, we further analyzed the impact of *pol32 Δ* on H3K4me3 and H3K56ac distribution at replicating DNA strands using eSPAN. Notably, H3K4me3 and H3K56ac eSPAN in *pol32 Δ* cells displayed a robust bias for the leading and lagging strand, respectively (Fig. 4, A to F), with a bias ratio more pronounced than *pol30-79*. Moreover, like in *pol30-79* cells, the leading strand bias of MNase-BrdU-IP-ssSeq peaks in *pol32 Δ* cells was stronger than the bias of sonication-BrdU-IP-ssSeq (Fig. 4, G to I), indicating that the leading strand bias of H3K4me3 eSPAN in *pol32 Δ* reflects a defect in parental histone transfer to lagging strands rather than in DNA synthesis.

Inspection of Pol32 protein sequence identified two stretches of amino acids resembling the histone binding motif found in Mcm2 and Pol1, respectively (Fig. 4J). The residues highlighted in red in Mcm2 and Pol1 are known to be critical for binding H3-H4 and affect parental histone transfer when mutated (25, 26). Therefore, we mutated the corresponding residues in Pol32 and tested how each mutant affects parental histone transfer. We found that the *pol32-2A2* mutation, but not *pol32-2A* mutation, impaired parental histone transfer based on analysis of H3K4me3 and H3K56ac at DNA replication forks using the eSPAN (Fig. 4K and fig. S5, A to C). Unlike *pol32 Δ* mutant cells, *pol32-2A2* mutant cells were not sensitive to hydroxyurea (HU), an inhibitor against ribonucleotide reductase and an agent inducing replication stress (Fig. 4L). We also noticed

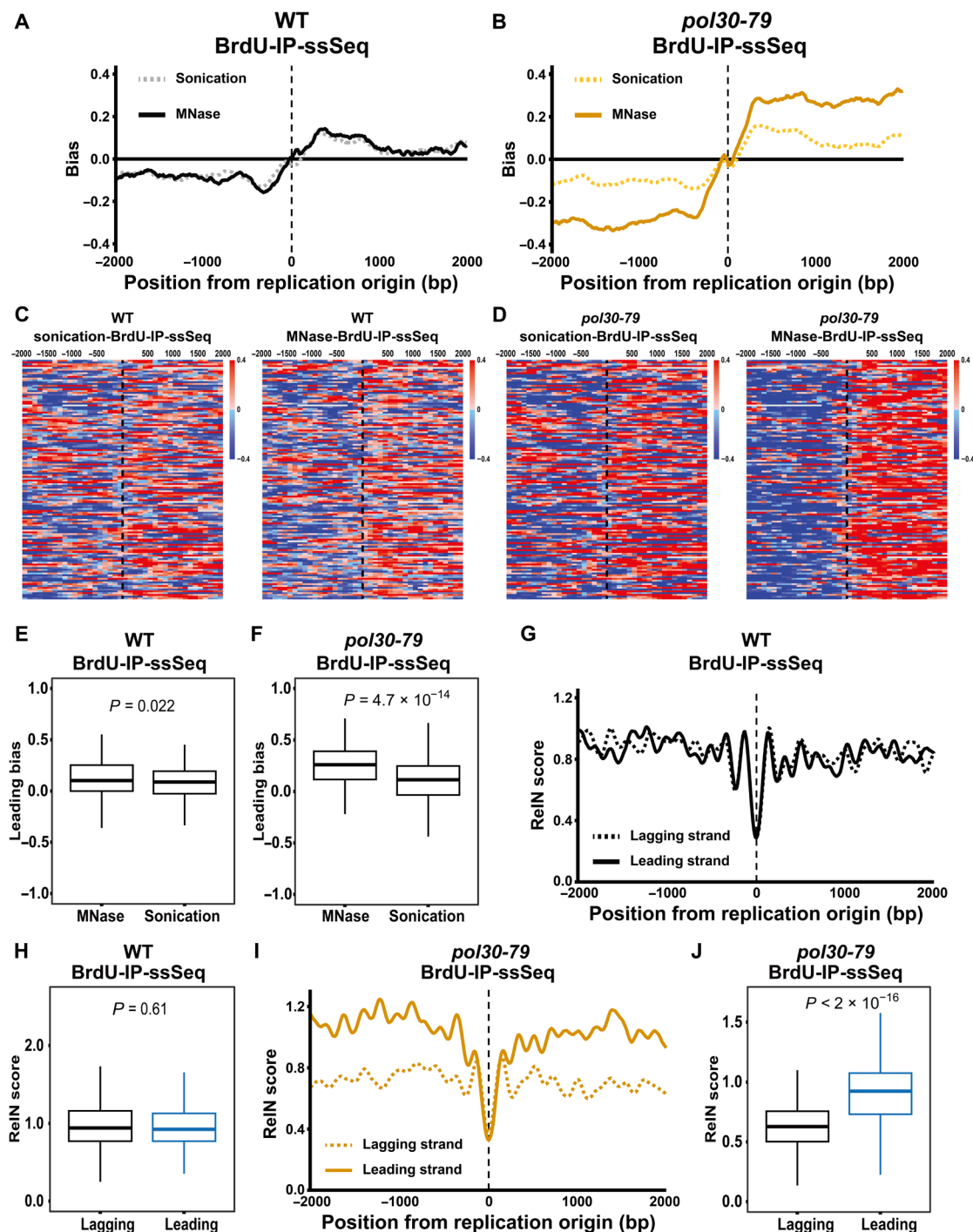


Fig. 2. Effects of the *pol30-79* mutation on DNA synthesis and nucleosome occupancy at nascent chromatin. (A and B) Average bias of sonication-BrdU-IP-ssSeq signals and MNase-BrdU-IP-ssSeq in WT (A) and *pol30-79* (B) cells at 134 early replication origins. Chromatin was sheared with sonication (sonication-BrdU-IP-ssSeq) or digested with MNase (MNase-BrdU-IP-ssSeq) before used for BrdU-IP and subsequent strand-specific sequencing. The bias was calculated using the formula: $(W - C)/(W + C)$, with an average of two biological replicates shown as mean \pm 95% confidence interval. (C and D) Heatmap of bias of sonication- and MNase-BrdU-IP-ssSeq signals in WT (C) and *pol30-79* cells (D). The BrdU-IP-ssSeq bias at each origin was calculated using the same formula in (A) and (B). Each row represents one origin. (E and F) Statistical analysis of leading strand bias at 134 early replication origins between MNase- and sonication-BrdU-IP-ssSeq in WT (E) and *pol30-79* cells (F). Each origin region was split into left fork and right fork to calculate their leading bias separately using the same formula in (A) and (B), which were then averaged to represent the leading bias of each origin. *P* values were calculated by Wilcoxon signed-rank test using two biological replicates. (G and I) Average RelN score in WT (G) and *pol30-79* (I) cells at leading and lagging strands of DNA replication forks of 134 early replication origins. Sequence reads mapped to leading or lagging strands were separated for the analysis. The average of two biological replicates is represented. (H and J) Statistical analysis of the RelN score at 134 early replication origins between lagging and leading strands in WT (H) and *pol30-79* cells (J). The RelN score was calculated the same way as (G) and (I), and the score flanking (−1000 and 1000 bp) of each origin was averaged. *P* values were calculated by Wilcoxon signed-rank test using two biological replicates.

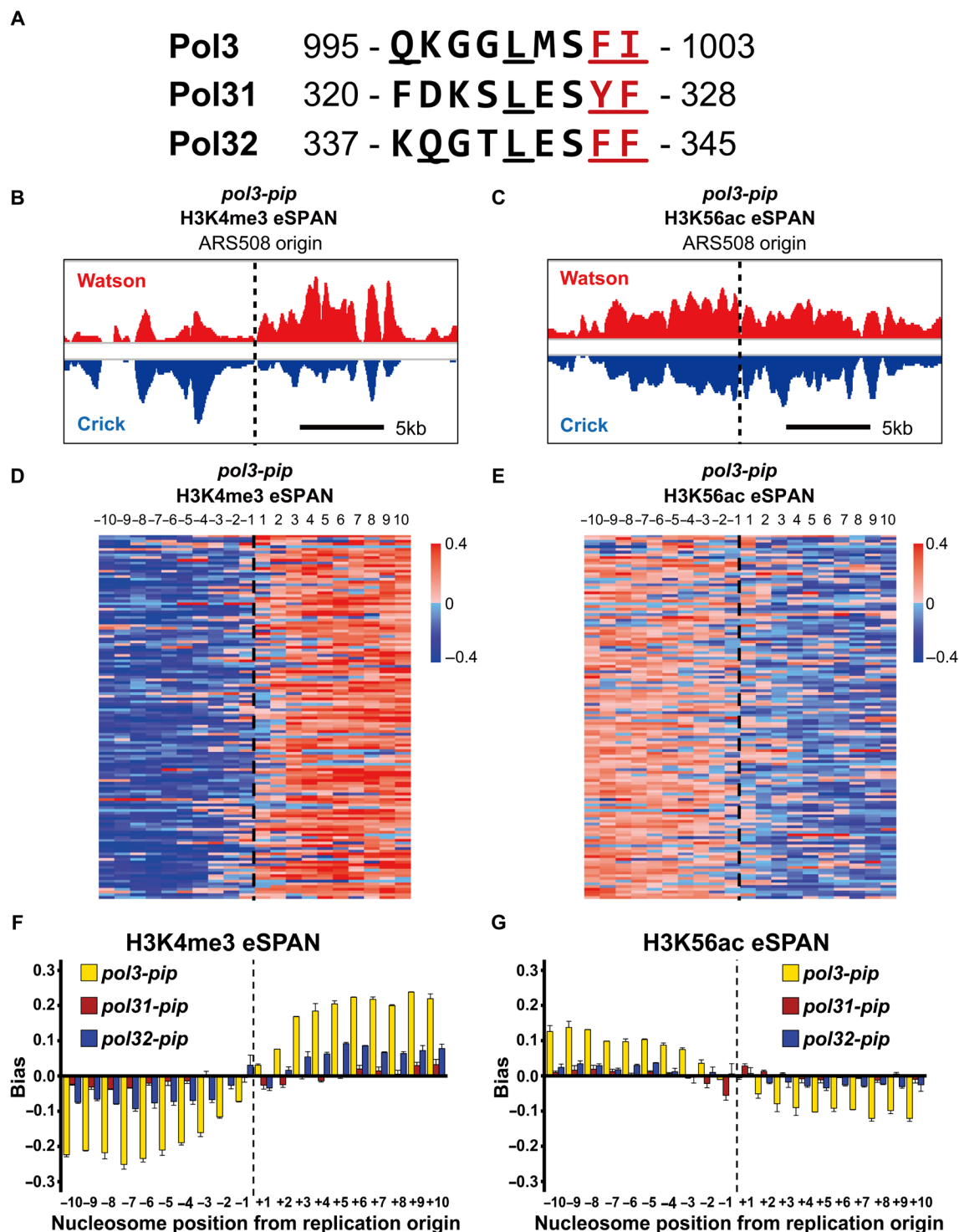


Fig. 3. DNA Pol δ is involved in the transfer of parental histone to lagging strands. (A) Amino acid sequence containing the residues that comprise the PIP motifs (underscored) in Pol3, Pol31, and Pol32. Red, residues substituted for alanines. (B and C) Snapshot of H3K4me3 (B) and H3K56ac (C) eSPAN at ARS508 in *pol3-pip* mutant cells with sequence reads of Watson and Crick strand indicated. (D and E) Heatmap of H3K4me3 (D) and H3K56ac (E) eSPAN bias at each of 20 individual nucleosomes surrounding each of 134 early replication origins in *pol3-pip* cells from two independent repeats, with each row representing one origin. (F and G) Average H3K4me3 (F) and H3K56ac (G) eSPAN signal bias from two independent repeats at 134 early replication origins in three strains with mutants with mutations at PIP box. Data are represented as mean + SEM from two independent repeats.

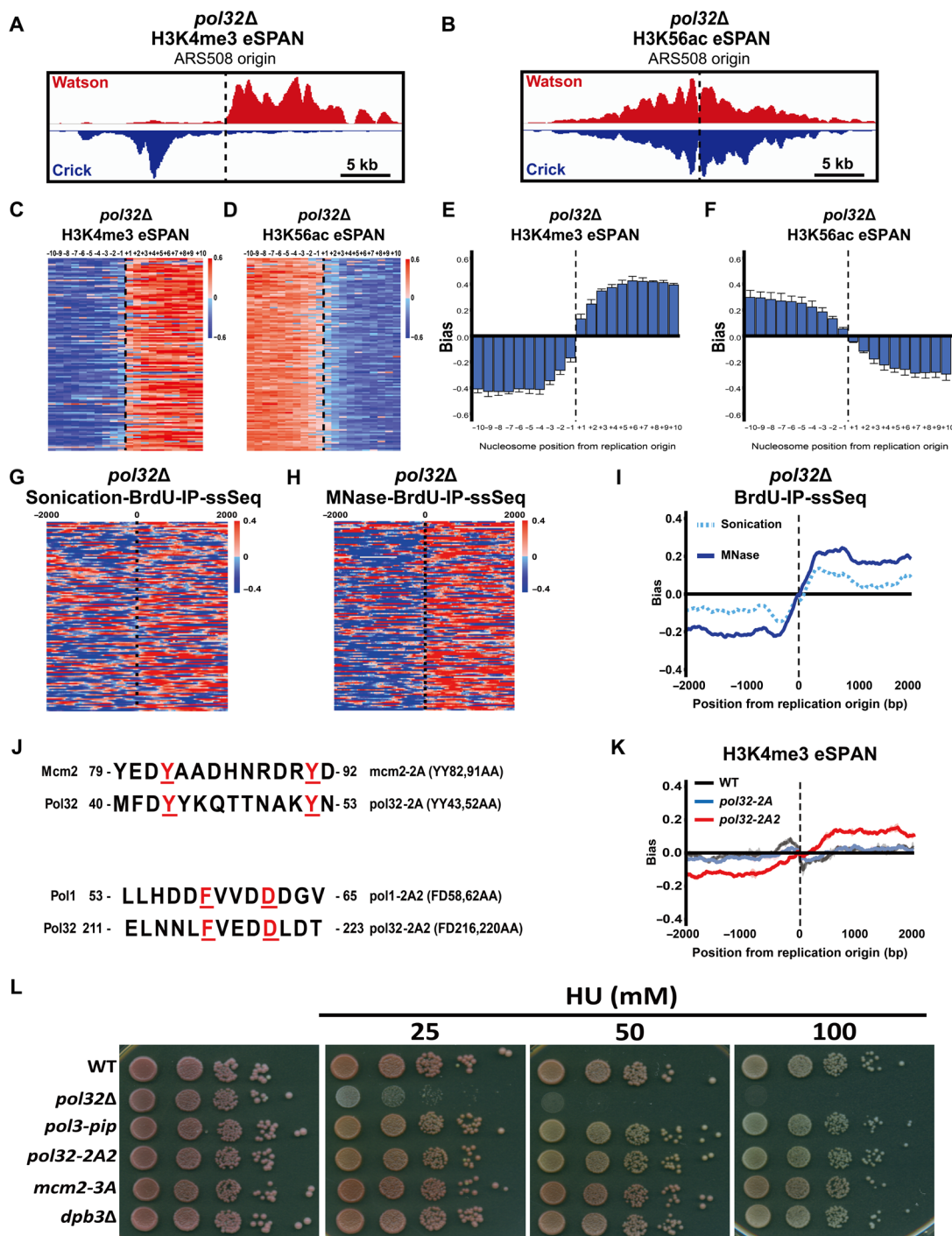


Fig. 4. Pol32 is involved in parental histone transfer to lagging strands. (A and B) Snapshots of H3K4me3 (A) and H3K56ac (B) eSPAN read density at ARS508 in *pol32Δ* cells. (C and D) Heatmap of H3K4me3 (C) and H3K56ac (D) eSPAN peak bias at each of the 20 nucleosomes surrounding each of the 134 early replication origins in *pol32Δ* cells. (E and F) Average H3K4me3 (E) or H3K56ac (F) eSPAN peak bias at each of the 20 nucleosomes surrounding 134 early-firing replication origins in *pol32Δ* cells, with mean \pm SEM of 2 shown. (G and H) Heatmap of sonication (G) and MNase (H) BrdU-IP-ssSeq signal bias at 4-kb regions surrounding each of 134 early-firing replication origins in *pol32Δ* cells. The bias was calculated using a slide window of 100 bp and using the formula: $(W - C)/(W + C)$. (I) Average of sonication-BrdU-IP-ssSeq and MNase-BrdU-IP-ssSeq signal bias at 4 kb surrounding 134 early replication origins in *pol32Δ* cells. The average of two biological replicates is represented as mean \pm 95% confidence interval. (J) The amino acid alignment of protein sequences in Pol32 that resemble the histone binding motif of Mcm2 and Pol. Mutations at residues highlighted in red in Mcm2 and mutations reduce the ability of Mcm2 and Pol1 to bind histone. (K) Average of H3K4me3 eSPAN bias calculated using a sliding window at 4-kb region surrounding 134 early replication origins in WT, *pol32-2A*, and *pol32-2A2* cells. The average of two biological replicates is represented as mean \pm 95% confidence interval. (L) The sensitivity to HU in strains of WT, *pol32Δ*, *pol3-pip*, *pol32-2A2*, *mcm2-3A*, and *dpb3Δ*. Tenfold serial dilutions of yeast cells were spotted onto plates without HU and with three different concentrations of HU.

that *pol3-pip* mutant cells were not sensitive to HU, like those of *mcm2-3A* and *dpb3Δ* cells known to be defective in parental histone transfer (Fig. 4L). Last, *pol32-2A2* mutant cells did not show detectable defects in DNA synthesis (fig. S5D). Of note, we could not be certain that the *pol32-2A* mutation affects histone binding despite repeated attempts. Now, we could not identify mutations in Pol δ that compromise its interactions with H3-H4 despite repeat attempts using multiple approaches, suggesting that it is likely that Pol δ interacts with H3-H4 through multiple interfaces at different subunits. Nonetheless, these results indicate that *pol32-2A* and *pol3-pip* mutations likely impair DNA synthesis in cells marginally at most. Together, these results provide additional support to the idea that Pol δ likely has a direct role in parental histone transfer in addition to its classical role in DNA synthesis.

Relationships between Mcm2 and the PCNA–Pol δ complex in parental histone transfer

Mutations at histone-binding domain of Mcm2 (*Mcm2-3A*) also result in a defect in the parental histone transfer to lagging strands (25). To discern the genetic relationship of *mcm2-3A*, *pol30-79*, *pol3-pip*, and *pol32Δ* on parental histone transfer, we compared nucleosome occupancy at nascent chromatin in these mutant strains using BrdU-IP-ssSeq with spike-in DNA from BrdU-labeled *Schizosaccharomyces pombe* cells (Fig. 5A). This allows us to normalize both sonication- and MNase-treated BrdU IP samples with spike-in DNA to obtain a normalized ReIN score (33). Using this method, we first analyzed the effects of *mcm2-3A* and *pol30-79* mutations on nucleosome occupancy at nascent chromatin. The *mcm2-3A* mutant showed a slightly but significantly reduced nucleosome occupancy at nascent chromatin compared to WT (Fig. 5, B and C). However, nucleosome occupancy at nascent chromatin in *pol30-79* was markedly lower than WT and *mcm2-3A* cells (Fig. 5, B and C). We noticed that the H3K4me3 eSPAN bias in *pol30-79* is not as pronounced as in *mcm2-3A*, suggesting that defects in DNA synthesis in *pol30-79*, not detected in *mcm2-3A* cells, may also contribute to the reduced total nucleosome occupancy on nascent chromatin in *pol30-79* cells. Because of the growth defects of the *mcm2-3A pol30-79* mutant cells, we could not obtain reliable and consistent ReIN score in these double-mutant cells from multiple independent repeats. We also observed that the *pol3-pip* mutation slightly but significantly reduced nucleosome occupancy on nascent chromatin, with additional defects detected in *pol3-pip mcm2-3A* double-mutant cells (Fig. 5, D and E). Similarly, deletion of *POL32* resulted in a reduced nucleosome occupancy at nascent chromatin, which became even more pronounced in the *mcm2-3A pol32Δ* double-mutant cells than either single mutant alone (fig. S6, A and B). Together, these results indicate that mutations at Mcm2, PCNA, and Pol3 impairing parental histone transfer also affect nucleosome occupancy on nascent chromatin and suggest that Pol δ likely functions in a pathway that is not completely overlapped with Mcm2 in the transfer of parental histones to lagging strands.

Pol δ interacts with H3-H4 and functions in heterochromatin silencing in budding yeast

We have shown previously that the non-essential subunits of DNA polymerase ϵ , Dpb3 and Dpb4, bind to H3-H4 histones (24). Moreover, mass spectrometry analysis indicates that Pol δ copurified with H3-tandem affinity purification (TAP) or H4-TAP (38). Therefore, we hypothesized that DNA Pol δ might have histone-binding capabilities to help shuttle H3-H4 tetramers to the lagging strand in a

manner similar to DNA polymerase ϵ for the leading strand. To test this idea, we first performed glutathione S-transferase (GST) pull-down assays to study a possible interaction between DNA Pol δ and H3-H4 tetramers in vitro. As shown in Fig. 5E, Pol32 copurified with Pol3-GST but not with GST alone, indicating that DNA Pol δ complex remained stable during the purification process. Significantly more H3 was pulled down from GST-Pol3 than the GST control, even at high salt concentrations. Together, these results indicate that Pol δ interacts with H3-H4 in vitro, which, in turn, promotes parental H3-H4 transfer following DNA replication.

Last, we analyzed the effects of *pol32Δ* and *pol3-pip* alone and in combination with *mcm2-3A* mutation on silencing at the *HML* locus. We observed that like *pol30-79*, *pol32Δ* and *pol3-pip* mutations reduced heterochromatin silencing at the *HML* locus compared to WT cells (Fig. 4G and fig. S6C). Moreover, *mcm2-3A pol3-pip* mutant cells exhibited a significantly higher silencing loss than either *mcm2-3A* or *pol3-pip* mutant alone (Fig. 5G). Furthermore, as reported (30), *pol30-79 mcm2-3A* double-mutant cells also showed a marked loss of silencing compared to either *pol30-79* or *mcm2-3A* mutant alone (fig. S6D). The loss of *HML* silencing was not increased in *pol32Δ mcm2-3A* strain compared to either *pol32Δ* or *mcm2-3A* single mutant alone (fig. S6C), although the double-mutant cells showed a marked reduction in nucleosome occupancy on nascent chromatin. Together, these results indicate that Pol δ is important for the inheritance of heterochromatin silencing, likely through its impacts on parental histone transfer.

PCNA is important for nucleosome positioning at nascent chromatin

We observed that nucleosome positions on nascent lagging strands appears to be compromised in *pol30-79* mutant cells compared to leading strands (Fig. 2I). To systematically analyze the effects of *pol30-79* on nucleosome position, we used “Nucleosome Dynamics,” a latest tool to analyze nucleosome dynamics (39) and analyzed nucleosome position surrounding acetyl-coenzyme A synthase (ACS) of total DNA (input) and BrdU-IP samples digested with MNase in WT, *mcm2-3A* and *pol30-79*. As shown in Fig. 6 (A and B), there was a slight shift in nucleosome position based on analysis of input samples of *pol30-79* compared to those of WT. The changes in nucleosome position in *pol30-79* cells compared to WT were much more evident when MNase-BrdU-IP-ssSeq samples, which measure nucleosome occupancy and positions at nascent chromatin, were analyzed (Fig. 6, C and D). In contrast, *mcm2-3A* mutation did not have apparent effects on nucleosome positioning (Fig. 6, A and C). These results suggest that the *pol30-79* mutation affects nucleosome positioning at nascent chromatin. To test this idea further, we analyzed the percentage of well-positioned nucleosomes surrounding ACS in WT, *mcm2-3A*, and *pol30-79* cells using both input and MNase-BrdU-IP-ssSeq samples. In general, we observed that the percentage of well-positioned nucleosomes determined by input samples was markedly higher than the corresponding BrdU-IP-ssSeq samples, consistent with the idea that nucleosome positioning at nascent chromatin is likely disrupted following DNA replication and could be restored afterward (Fig. 6, E and F). Furthermore, the percentage of well-positioned nucleosomes of input samples was similar among WT, *mcm2-3A*, and *pol30-79* samples (Fig. 6C). In contrast, the percentage of well-positioned nucleosomes at nascent chromatin in *pol30-79* cells was significantly lower than WT cells, whereas *mcm2-3A* mutant cells had similar amounts well-positioned nucleosomes at

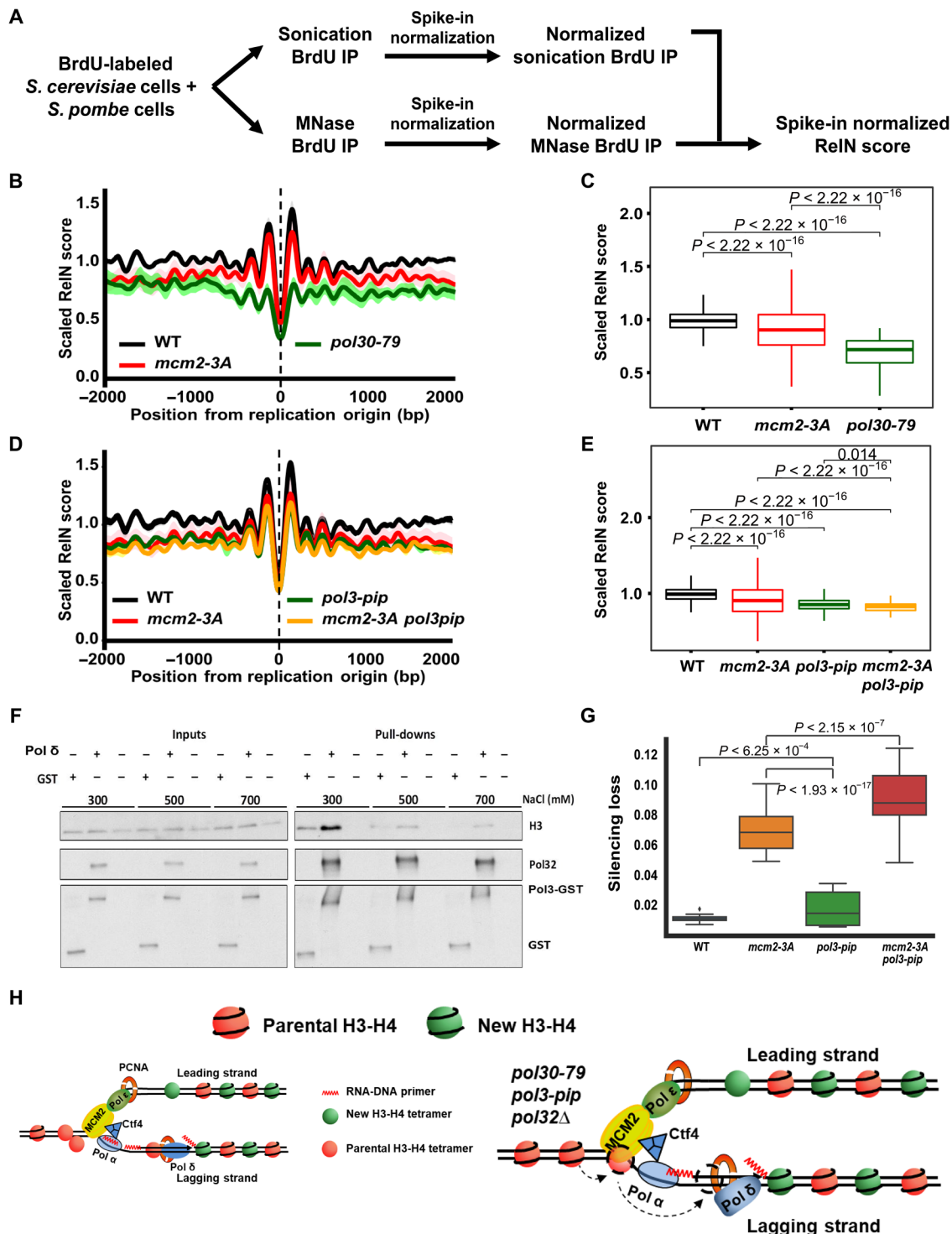


Fig. 5. Pol δ interacts with H3-H4 and functions non-overlappingly with Mcm2 in parental histone transfer. (A) An outline for calculating normalized ReIN-score. (B and C) Effects of *pol30-79* and *mcm2-3A* mutations on nucleosome occupancy at nascent chromatin. The average ReIN score at early replication origins in mutant strains was calculated on the basis of the outline in (A) and scaled to WT strain for comparison. Data in (B) are represented as mean \pm 95% confidence interval. The average scaled ReIN score from -1 to $+1$ kb of 134 early replication origins was presented as boxplot with P values calculated by t test (C). (D and E) Effects of *pol3-pip* and *mcm2-3A* mutation alone and in combination on nucleosome occupancy at nascent chromatin. (F) Pol δ interacts with H3-H4 in vitro. GST-Pol3-Pol31-Pol32 and GST were used to pull-down H3-H4 tetramers at different salt concentrations, and bound proteins were analyzed by Western blot using the indicated antibodies. (G) Effects of *pol3-pip* alone and in combination with *mcm2-3A* on silencing at the *HML* locus. (H) A model for the role of the PCNA-Pol δ complex in parental histone transfer. Pol δ deposits a parental H3-H4 tetramer on an Okazaki fragment only when it reaches the nucleosome on the preceding Okazaki fragment. In this way, parental H3-H4 tetramers can be transferred to right positions along the DNA on lagging strands.

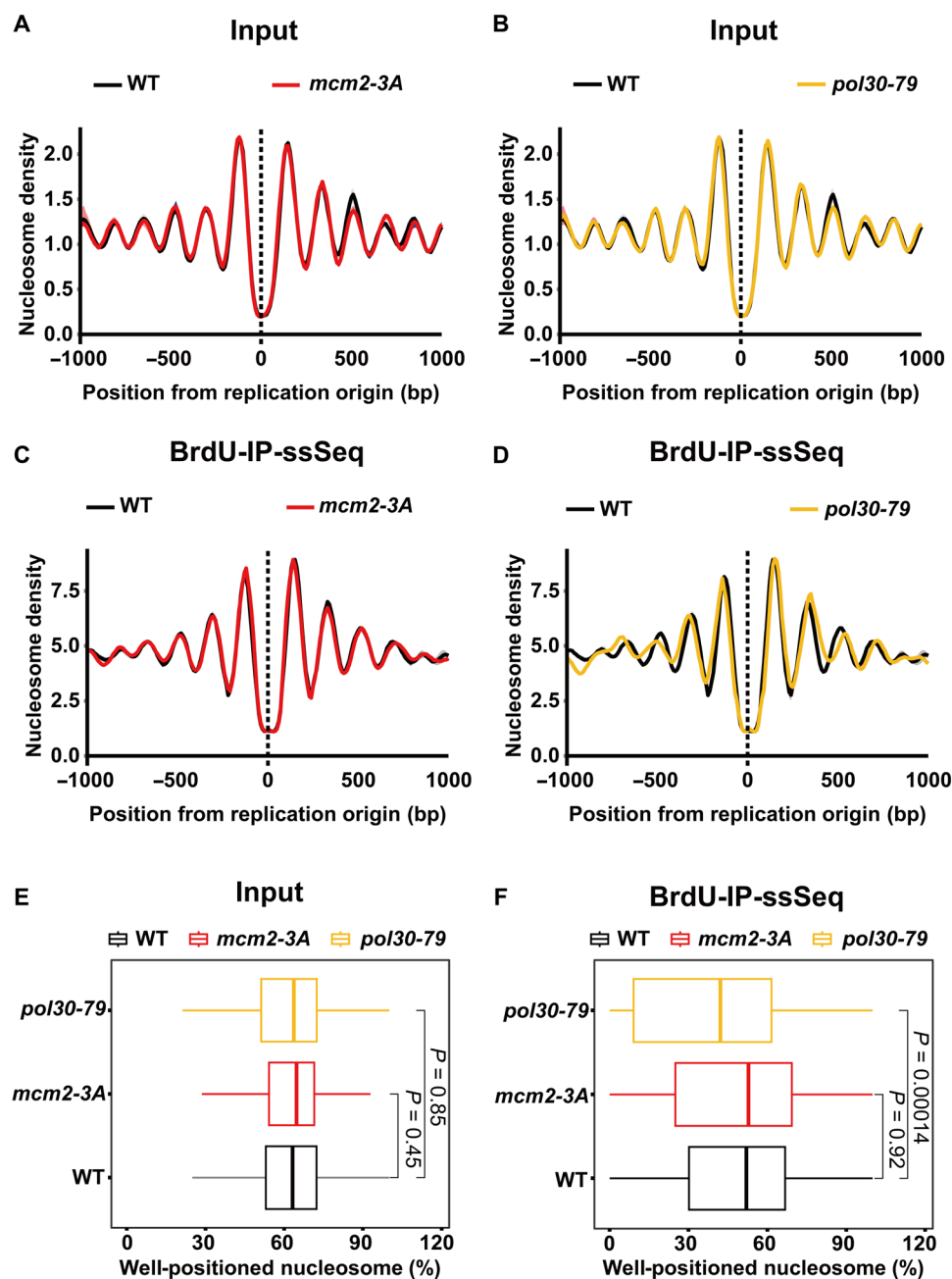


Fig. 6. PCNA is important for nucleosome position at nascent chromatin. (A to D) Average of nucleosome density at 2-kb regions surrounding 139 ACS sites defined by Eaton *et al.* (49) of the input samples [WT and *mcm2-3A* (A) and WT and *pol30-79* (B)] and MNase-BrdU-IP-ssSeq samples [WT and *mcm2-3A* (C) and WT and *pol30-79* (D)]. The average of two biological replicates was represented as mean \pm 95% confidence interval. (E and F) Percentage of well-positioned nucleosomes of input (E) and MNase-BrdU-IP-ssSeq (F) samples at 127 shared replicated regions from WT, *mcm2-3A*, and *pol30-79* strains. P values were calculated by Wilcoxon signed-rank test. Well-positioned nucleosomes at each strain surrounding 139 ACS sites were calculated as described in the experimental procedures and normalized against total nucleosomes in the regions.

nascent chromatin compared to WT (Fig. 6D). Together, these results reveal a previously unknown role of PCNA in nucleosome positioning at nascent chromatin. Because *mcm2-3A* mutation also compromises parental histone transfer to lagging strands, these results also suggest that the effects of *pol30-79* on nucleosome positioning at nascent chromatin may not be directly linked to its impact on the transfer of parental histones.

We also performed the same analysis on the effects of *pol3-pip* and *pol32A* on nucleosome positioning using both input and BrdU-IP-ssSeq samples. We found that the *pol3-pip* mutation did not have a significant impact on nucleosome positions as measured using both input and BrdU-IP-ssSeq samples (fig. S7). In contrast, the *pol32A* mutation slightly affected nucleosome positions, and the percentage of well-positioned nucleosomes of nascent chromatin

(BrdU-IP-ssSeq samples) was reduced slightly in *pol32Δ* cells compared to WT cells (fig. S7D). The percentage of well-positioned nucleosomes increased in the input samples of *pol32Δ* compared to WT cells. Now, we do not know the discordance between the input and BrdU samples of *pol32Δ* cells. Because the H3K4me3 eSPAN bias in *pol32Δ* cells is larger than that of *pol30-79* cells (Figs. 1 and 4), these results provide additional support to the idea that the effects of *pol30-79* on nucleosome position at nascent chromatin may not be directly linked to its impact on parental histone transfer.

DISCUSSION

PCNA, a protein known to mediate nucleosome assembly of new H3-H4, also regulates parental histone transfer

PCNA is essential for DNA replication and DNA repair. Here, we show that PCNA also plays an important role in regulating the transfer of parental histones H3-H4 to lagging strands of DNA replication forks. Using the eSPAN method that can monitor the distribution of parental H3K4me3 and new H3K56ac at replicating DNA strands, we found that the PCNA mutant *pol30-79* shows defects in the transfer of parental histones to lagging strands of DNA replication forks. The residues mutated in the *pol30-79* are located at the interdomain connecting loop where many proteins involved in DNA replication including DNA polymerases and enzymes involved in the processing and maturation of Okazaki fragments bind (23). Therefore, it is possible that defects in parental histone transfer in *pol30-79* mutant cells arise from DNA synthesis defects. We present multiple lines of evidence indicating that this is unlikely the case despite the fact that we could not completely rule out this possibility. First, we found that the effect of *pol30-79* mutant on DNA synthesis is less than that of *pol30-6* mutant based on analysis of DNA synthesis by BrdU-IP-ssSeq, which can measure relative amount of leading and lagging strand DNA synthesis (fig. S2A). Consistent with this result, previous studies indicate that the *pol30-6* mutation impairs the PCNA's ability to stimulate Pol δ activity more than *pol30-79* in vitro. Furthermore, the *pol30-6* mutant cells are much more sensitive to DNA damage agents than *pol30-79* cells (30, 31). However, the *pol30-6* mutant cells did not exhibit defects in parental histone transfer to lagging strand as in *pol30-79* cells. Second, H3K4me3 eSPAN signals in each sample including *pol30-79* mutation were normalized against corresponding BrdU-IP-ssSeq signals. Therefore, the impact of DNA synthesis defects induced by *pol30-79* mutation on the eSPAN bias was in principle minimized. Third, we compared BrdU-IP-ssSeq signals in WT and *pol30-79* cells using chromatin sheared by sonication (sonication-BrdU-IP-ssSeq) to that prepared by digestion with MNase (MNase-BrdU-IP-ssSeq). In WT cells, we found that sonication- and MNase-BrdU-IP-ssSeq signals were similar, consistent with the idea that DNA replication is coupled to nucleosome assembly in WT cells. In contrast, in *pol30-79* cells, MNase-BrdU-IP-ssSeq signals at lagging strands were reduced significantly compared to those of sonication-BrdU-IP-ssSeq (Fig. 2B), an indication for defects in nucleosome assembly. Last, nucleosome occupancy at lagging strands is reduced compared to leading strand in *pol30-79* cells based on analysis of nucleosome occupancy on nascent chromatin using ReIN-Map (Fig. 2E). All these results indicate that nucleosome assembly on nascent chromatin is defective in *pol30-79* cells compared to WT cells, supporting the idea that PCNA regulates the transfer of parental histones to lagging strands at DNA replication forks.

In both yeast and mammalian cells, it has been shown that PCNA interacts with CAF-1 (17, 19, 22), the classic histone chaperone involved in the deposition of newly synthesized H3-H4 onto replicating DNA for nucleosome formation. Furthermore, we have shown that *pol30-8* mutant allele affects CAF-1-mediated nucleosome assembly pathway in budding yeast (19). More recently, it has been shown that mouse ES cells with the same PCNA mutation (PCNA-8) as the yeast *pol30-8* mutation also reduces the PCNA-CAF-1 interaction, and PCNA-8 mouse ES cells show similar phenotypes as deletion of CAF-1/p150 in terms of growth and differentiation. Last, the homozygous PCNA-8 mutation is embryonic lethal (40), a phenotype shared by knockout CAF-1 p150 (41). Together, these results indicate that the effect of *pol30-8* mutation on CAF-1-nucleosome assembly is conserved from yeast to mammalian cells. However, the *pol30-8* mutant allele has little impacts on the transfer of parental histones onto replicating DNA strands in budding yeast (Fig. 1). Residues mutated in *pol30-8* and *pol30-79* are localized at different surfaces of PCNA (Fig. 1A). Therefore, it is possible that PCNA uses these two different surfaces to bind different proteins (CAF-1 and Pol δ) to coordinate the transfer of parental histones and deposition of new H3-H4, two pathways that are critical for the assembly of replicating DNA into nucleosomes.

The PCNA-Pol δ complex couples lagging strand DNA synthesis to parental histone transfer

How does PCNA regulate the parental histone transfer? PCNA interacts with several proteins involved in lagging strand DNA synthesis, processing, and maturation. We have provided evidence supporting the idea that PCNA regulates the transfer of parental histones to lagging strands via its interaction with Pol δ . By analyzing mutations at the PIP box of each of the Pol δ subunit, we found that mutations at the PIP box of Pol3 and, to lesser extent, Pol32, affected the parental histone transfer to lagging strands. Moreover, deletion of *POL32*, which is not essential, also affects parental histone transfer to lagging strands. In contrast, mutations at the PIP box of Pol31, another subunit of Pol δ , have no apparent effects on parental histone transfer. Furthermore, depletion/deletion of two other proteins (Rad27 and Dna2), which interact with PCNA for lagging strand processing, as well as Elg1, a PCNA unloader, does not affect parental histone transfer. Last, we identified that a *pol32-2A2* mutant, with mutations at the region resembling the histone binding motif of Pol1, affects parental histone transfer. Unlike *pol32Δ* mutant cells, the *pol32-2A2* mutant cells were not sensitive to HU, suggesting that this mutation has little impact on DNA synthesis in vivo. Of note, we could not be certain that the *pol32-2A2* mutation affects histone binding. Nonetheless, this separation of function of *pol32* mutant provides additional evidence that Pol δ has a role in parental histone transfer.

Lagging strand DNA synthesis involves repeated cycles of RNA-DNA primer synthesis by Pol α , strand displacement synthesis by Pol δ for the generation of 5'-RNA flap of the proceeding Okazaki fragment, and the subsequent removal of the RNA-DNA primer for the ligation of Okazaki fragments. Nucleosome assembly during S phase is intrinsically coupled to lagging strand DNA synthesis by unknown mechanisms (32). Furthermore, multiple lines of evidence suggest that nucleosomes are already formed on Okazaki fragments before processing and ligation. For instance, purified Okazaki fragments before ligation are sized like nucleosome repeats (32), and Fen1 and DNA ligase 1 can process and ligate nucleosomal substrates

efficiently (42, 43). In addition, the nucleosome on the proceeding Okazaki fragment likely acts as a barrier to prevent Pol δ from excessive strand displacement synthesis (32). Therefore, it is not unexpected that Fen 1 and DNA2 mutant cells, which are only defective in the processing of Okazaki fragments, do not affect parental histone transfer (fig. S2). Therefore, we speculate that Pol δ deposits a parental H3-H4 tetramer on an Okazaki fragment only when it reaches the nucleosome on the proceeding Okazaki fragment. In addition to its role in DNA replication, the PCNA–Pol δ complex is involved in break-induced DNA replication and DNA repair (44, 45). Because chromatin states, like those in DNA replication, need to be maintained following DNA repair (46), we suggest that the PCNA–Pol δ complex may also function in parental histone recycling in DNA repair.

Previously, we have shown that Mcm2–Ctf4–Pol α axis promotes the parental histone transfer to lagging strands. Through analysis of nucleosome occupancy at nascent chromatin in *mcm2-3A* mutant cells alone and in combination with *pol3-pip* mutant and *pol32 Δ* , we found that the PCNA–Pol δ axis and Mcm2 likely regulate parental histone transfer not only in overlapping but also independent pathways. PCNA–Pol δ replaces Pol α for the synthesis of Okazaki fragments. We suggest that parental histones passage through Mcm2–Ctf4 Pol α first and to PCNA–Pol δ and other proteins before assembled into nucleosomes at Okazaki fragment. Moreover, like Mcm2, Dpb3–Dpb4, and Pol1 that can bind H3-H4, Pol δ also interacts with H3-H4 in vitro. Therefore, multiple replisome components are involved in the transfer of parental histones to replicated DNA for nucleosome assembly. In the future, it would be interesting to determine how these pathways coordinate for faithful transfer of parental histones for epigenetic memory and how Pol δ interacts with histones.

A role for PCNA in nucleosome position

We found that nucleosome positions at nascent chromatin in *pol30-79* mutant cells are altered. Furthermore, the number of well-positioned nucleosomes at nascent chromatin is reduced in the mutant cells compared to WT cells. Unexpectedly, we did not observe a marked defect in nucleosome position in *mcm2-3A*, *pol3-pip*, and *pol32 Δ* mutant cells, all of which impair parental histone transfer to lagging strand to a degree similar or larger than the *pol30-79* cells. Previously, it has been shown that parental histones H3 can memorize their nucleosome positions along the DNA following DNA replication (14), likely through the aid of chromatin remodelers (47). Furthermore, in *mcm2-3A* mutant cells, no local movement of nucleosomes following DNA replication was detected. However, the number of nucleosomes is reduced in *mcm2-3A* mutant cells alone and when combined with *dpb3 Δ* cells (14). These results obtained using independent assays were consistent with our analysis of the impact of *mcm2-3A* mutation on nucleosome positions. Therefore, the effects of *pol30-79* on nucleosome positioning are unlikely due to its impact on parental histone transfer. We suggest that PCNA may interact with chromatin remodelers (47, 48) to facilitate nucleosome positioning at nascent chromatin, a hypothesis that will be tested in future studies. Furthermore, it would be interesting to determine the functional significance of the impact of PCNA on nucleosome positioning.

Limitation of the study

While we presented multiple lines of evidence indicating that the defects in parental histone transfer in *pol30-79*, *pol3-pip*, and *pol32 Δ*

mutant cells are unlikely due to defects in lagging strand DNA synthesis in these mutant cells, we cannot completely exclude this possibility. Nonetheless, the fact that the PCNA–DNA Pol δ interaction is important for faithful segregation of nucleosomes at replication forks suggests that the stimulation of DNA synthesis processivity of Pol δ by PCNA allows for the timely deposition of parental histones onto lagging strands.

MATERIALS AND METHODS

For more information regarding the experimental design, see “Experimental procedures” in the Supplementary Materials.

Supplementary Materials

This PDF file includes:

Experimental procedures
Figs. S1 to S7
Tables S1 and S2
References

REFERENCES AND NOTES

1. D. Reinberg, L. D. Vales, Chromatin domains rich in inheritance. *Science* **361**, 33–34 (2018).
2. A. V. Probst, E. Dunleavy, G. Almouzni, Epigenetic inheritance during the cell cycle. *Nat. Rev. Mol. Cell Biol.* **10**, 192–206 (2009).
3. K. Luger, A. W. Mader, R. K. Richmond, D. F. Sargent, T. J. Richmond, Crystal structure of the nucleosome core particle at 2.8 Å resolution. *Nature* **389**, 251–260 (1997).
4. B. J. Lesch, Z. Tothova, E. A. Morgan, Z. Liao, R. T. Bronson, B. L. Ebert, D. C. Page, Intergenerational epigenetic inheritance of cancer susceptibility in mammals. *eLife* **8**, e39380 (2019).
5. A. Serra-Cardona, Z. Zhang, Replication-coupled nucleosome assembly in the passage of epigenetic information and cell identity. *Trends Biochem. Sci.* **43**, 136–148 (2018).
6. M. Ransom, B. K. Dennehey, J. K. Tyler, Chaperoning histones during DNA replication and repair. *Cell* **140**, 183–195 (2010).
7. K. R. Stewart-Morgan, N. Petryk, A. Groth, Chromatin replication and epigenetic cell memory. *Nat. Cell Biol.* **22**, 361–371 (2020).
8. M. Xu, C. Long, X. Chen, C. Huang, S. Chen, B. Zhu, Partitioning of histone H3-H4 tetramers during DNA replication-dependent chromatin assembly. *Science* **328**, 94–98 (2010).
9. K. Ragunathan, G. Jih, D. Moazed, Epigenetics. Epigenetic inheritance uncoupled from sequence-specific recruitment. *Science* **348**, 1258699 (2015).
10. X. Wang, D. Moazed, DNA sequence-dependent epigenetic inheritance of gene silencing and histone H3K9 methylation. *Science* **356**, 88–91 (2017).
11. R. T. Coleman, G. Struhl, Causal role for inheritance of H3K27me3 in maintaining the OFF state of a *Drosophila* HOX gene. *Science* **356**, eaai8236 (2017).
12. N. Liu, Z. Zhang, H. Wu, Y. Jiang, L. Meng, J. Xiong, Z. Zhao, X. Zhou, J. Li, H. Li, Y. Zheng, S. Chen, T. Cai, S. Gao, B. Zhu, Recognition of H3K9 methylation by GLP is required for efficient establishment of H3K9 methylation, rapid target gene repression, and mouse viability. *Genes Dev.* **29**, 379–393 (2015).
13. S. I. S. Grewal, The molecular basis of heterochromatin assembly and epigenetic inheritance. *Mol. Cell* **83**, 1767–1785 (2023).
14. G. Schlissel, J. Rine, The nucleosome core particle remembers its position through DNA replication and RNA transcription. *Proc. Natl. Acad. Sci. U.S.A.* **116**, 20605–20611 (2019).
15. T. M. Escobar, O. Oksuz, R. Saldaña-Meyer, N. Descostes, R. Bonasio, D. Reinberg, Active and repressed chromatin domains exhibit distinct nucleosome segregation during DNA replication. *Cell* **179**, 953–963.e11 (2019).
16. S. Nakano, B. Stillman, H. R. Horvitz, Replication-coupled chromatin assembly generates a neuronal bilateral asymmetry in *C. elegans*. *Cell* **147**, 1525–1536 (2011).
17. K. Shibahara, B. Stillman, Replication-dependent marking of DNA by PCNA facilitates CAF-1-coupled inheritance of chromatin. *Cell* **96**, 575–585 (1999).
18. A. Verreault, P. D. Kaufman, R. Kobayashi, B. Stillman, Nucleosome assembly by a complex of CAF-1 and acetylated histones H3/H4. *Cell* **87**, 95–104 (1996).
19. Z. Zhang, K. Shibahara, B. Stillman, PCNA connects DNA replication to epigenetic inheritance in yeast. *Nature* **408**, 221–225 (2000).
20. H. Tagami, D. Ray-Gallet, G. Almouzni, Y. Nakatani, Histone H3.1 and H3.3 complexes mediate nucleosome assembly pathways dependent or independent of DNA synthesis. *Cell* **116**, 51–61 (2004).

21. C. P. Liu, Z. Yu, J. Xiong, J. Hu, A. Song, D. Ding, C. Yu, N. Yang, M. Wang, J. Yu, P. Hou, K. Zeng, Z. Li, Z. Zhang, X. Zhang, W. Li, Z. Zhang, B. Zhu, G. Li, R. M. Xu, Structural insights into histone binding and nucleosome assembly by chromatin assembly factor-1. *Science* **381**, eadd8673 (2023).
22. J. G. Moggs, P. Grandi, J. P. Quivy, Z. O. Jónsson, U. Hübscher, P. B. Becker, G. Almouzni, A CAF-1-PCNA-mediated chromatin assembly pathway triggered by sensing DNA damage. *Mol. Cell. Biol.* **20**, 1206–1218 (2000).
23. K. N. Choe, G.-L. Moldovan, Forging ahead through darkness: PCNA, still the principal conductor at the replication fork. *Mol. Cell* **65**, 380–392 (2017).
24. C. Yu, H. Gan, A. Serra-Cardona, L. Zhang, S. Gan, S. Sharma, E. Johansson, A. Chabes, R. M. Xu, Z. Zhang, A mechanism for preventing asymmetric histone segregation onto replicating DNA strands. *Science* **361**, 1386–1389 (2018).
25. H. Gan, A. Serra-Cardona, X. Hua, H. Zhou, K. Labib, C. Yu, Z. Zhang, The Mcm2-Ctf4-Pol α axis facilitates parental histone H3-H4 transfer to lagging strands. *Mol. Cell* **72**, 140–151.e3 (2018).
26. Z. Li, X. Hua, A. Serra-Cardona, X. Xu, S. Gan, H. Zhou, W. S. Yang, C. L. Chen, R. M. Xu, Z. Zhang, DNA polymerase α interacts with H3-H4 and facilitates the transfer of parental histones to lagging strands. *Sci. Adv.* **6**, eabb5820 (2020).
27. N. Petryk, M. Dalby, A. Wenger, C. B. Stromme, A. Strandsby, R. Andersson, A. Groth, MCM2 promotes symmetric inheritance of modified histones during DNA replication. *Science* **361**, 1389–1392 (2018).
28. S. Waga, B. Stillman, The DNA replication fork in eukaryotic cells. *Annu. Rev. Biochem.* **67**, 721–751 (1998).
29. C. Yu, H. Gan, J. Han, Z. X. Zhou, S. Jia, A. Chabes, G. Farrugia, T. Ordog, Z. Zhang, Strand-specific analysis shows protein binding at replication forks and PCNA unloading from lagging strands when forks stall. *Mol. Cell* **56**, 551–563 (2014).
30. R. Ayyagari, K. J. Impellizzeri, B. L. Yoder, S. L. Gary, P. M. Burgers, A mutational analysis of the yeast proliferating cell nuclear antigen indicates distinct roles in DNA replication and DNA repair. *Mol. Cell. Biol.* **15**, 4420–4429 (1995).
31. J. C. Eisenberg, R. Ayyagari, X. V. Gomes, P. M. Burgers, Mutations in yeast proliferating cell nuclear antigen define distinct sites for interaction with DNA polymerase delta and DNA polymerase epsilon. *Mol. Cell. Biol.* **17**, 6367–6378 (1997).
32. D. J. Smith, I. Whitehouse, Intrinsic coupling of lagging-strand synthesis to chromatin assembly. *Nature* **483**, 434–438 (2012).
33. S. Liu, Z. Xu, H. Leng, P. Zheng, J. Yang, K. Chen, J. Feng, Q. Li, RPA binds histone H3-H4 and functions in DNA replication-coupled nucleosome assembly. *Science* **355**, 415–420 (2017).
34. T. Kubota, Y. Katou, R. Nakato, K. Shirahige, A. D. Donaldson, Replication-coupled PCNA unloading by the Elg1 complex occurs genome-wide and requires okazaki fragment ligation. *Cell Rep.* **12**, 774–787 (2015).
35. R. Janke, G. A. King, M. Kupiec, J. Rine, Pivotal roles of PCNA loading and unloading in heterochromatin function. *Proc. Natl. Acad. Sci. U.S.A.* **115**, E2030–E2039 (2018).
36. E. Johansson, P. Garg, P. M. J. Burgers, The Pol32 subunit of DNA polymerase δ contains separable domains for processive replication and proliferating cell nuclear antigen (PCNA) binding. *J. Biol. Chem.* **279**, 1907–1915 (2004).
37. N. Acharya, R. Klassen, R. E. Johnson, L. Prakash, S. Prakash, PCNA binding domains in all three subunits of yeast DNA polymerase δ modulate its function in DNA replication. *Proc. Natl. Acad. Sci. U.S.A.* **108**, 17927–17932 (2011).
38. J. M. Gilmore, M. E. Sardiu, S. Venkatesh, B. Stutzman, A. Peak, C. W. Seidel, J. L. Workman, L. Florens, M. P. Washburn, Characterization of a highly conserved histone related protein, Ydl156w, and its functional associations using quantitative proteomic analyses. *Mol. Cell. Proteomics* **11**, M111.011544 (2012).
39. D. Buitrago, L. Codó, R. Illa, P. de Jorge, F. Battistini, O. Flores, G. Bayarri, R. Royo, M. del Pino, S. Heath, A. Hospital, J. L. Gelpi, I. B. Heath, M. Orozco, Nucleosome Dynamics: A new tool for the dynamic analysis of nucleosome positioning. *Nucleic Acids Res.* **47**, 9511–9523 (2019).
40. L. Cheng, X. Zhang, Y. Wang, H. Gan, X. Xu, X. Lv, X. Hua, J. Que, T. Ordog, Z. Zhang, Chromatin assembly factor 1 (CAF-1) facilitates the establishment of facultative heterochromatin during pluripotency exit. *Nucleic Acids Res.* **47**, 11114–11131 (2019).
41. M. Houlard, S. Berlivet, A. V. Probst, J. P. Quivy, P. Héry, G. Almouzni, M. Gérard, CAF-1 is essential for heterochromatin organization in pluripotent embryonic cells. *PLOS Genet.* **2**, e181 (2006).
42. D. R. Chafin, J. M. Vitolo, L. A. Henriksen, R. A. Bambara, J. J. Hayes, Human DNA ligase I efficiently seals nicks in nucleosomes. *EMBO J.* **19**, 5492–5501 (2000).
43. C. F. Huggins, D. R. Chafin, S. Aoyagi, L. A. Henriksen, R. A. Bambara, J. J. Hayes, Flap endonuclease 1 efficiently cleaves base excision repair and DNA replication intermediates assembled into nucleosomes. *Mol. Cell* **10**, 1201–1211 (2002).
44. R. A. Donnianni, Z. X. Zhou, S. A. Lujan, A. al-Zain, V. Garcia, E. Glancy, A. B. Burkholder, T. A. Kunkel, L. S. Symington, DNA polymerase delta synthesizes both strands during break-induced replication. *Mol. Cell* **76**, 371–381.e4 (2019).
45. J. R. Lydeard, Z. Lipkin-Moore, Y. J. Sheu, B. Stillman, P. M. Burgers, J. E. Haber, Break-induced replication requires all essential DNA replication factors except those specific for pre-RC assembly. *Genes Dev.* **24**, 1133–1144 (2010).
46. U. Chakraborty, Z. J. Shen, J. Tyler, Chaperoning histones at the DNA repair dance. *DNA Repair* **108**, 103240 (2021).
47. C. Y. Zhou, S. L. Johnson, N. I. Gamarra, G. J. Narlikar, Mechanisms of ATP-dependent chromatin remodeling motors. *Annu. Rev. Biophys.* **45**, 153–181 (2016).
48. R. A. Poot, L. Bozhenok, D. L. C. van den Berg, S. Steffensen, F. Ferreira, M. Grimaldi, N. Gilbert, J. Ferreira, P. D. Varga-Weisz, The Williams syndrome transcription factor interacts with PCNA to target chromatin remodelling by ISWI to replication foci. *Nat. Cell Biol.* **6**, 1236–1244 (2004).
49. M. L. Eaton, K. Galani, S. Kang, S. P. Bell, D. M. MacAlpine, Conserved nucleosome positioning defines replication origins. *Genes Dev.* **24**, 748–753 (2010).
50. C. Noguchi, M. V. Garabedian, M. Malik, E. Noguchi, A vector system for genomic FLAG epitope-tagging in *Schizosaccharomyces pombe*. *Biotechnol. J.* **3**, 1280–1285 (2008).
51. M. F. Laughery, T. Hunter, A. Brown, J. Hoopes, T. Ostbye, T. Shumaker, J. J. Wyrick, New vectors for simple and streamlined CRISPR-Cas9 genome editing in *Saccharomyces cerevisiae*. *Yeast* **32**, 711–720 (2015).
52. M. J. Dunham, M. R. Gartenberg, G. W. Brown, *Methods in Yeast Genetics and Genomics: A Cold Spring Harbor Laboratory Course Manual*, (Cold Spring Harbor Laboratory Press, 2015).
53. H. Gan, C. Yu, S. Devbhandari, S. Sharma, J. Han, A. Chabes, D. Remus, Z. Zhang, Checkpoint kinase Rad53 couples leading- and lagging-strand DNA synthesis under replication stress. *Mol. Cell* **68**, 446–455.e3 (2017).
54. M. Wal, B. F. Pugh, Genome-wide mapping of nucleosome positions in yeast using high-resolution MNase ChIP-Seq. *Method Enzymol.* **513**, 233–250 (2012).
55. J. Han, H. Zhou, B. Horazdovsky, K. Zhang, R. M. Xu, Z. Zhang, Rtt109 acetylates histone H3 lysine 56 and functions in DNA replication. *Science* **315**, 653–655 (2007).
56. J. D. Nelson, O. Denisenko, K. Bomsztyk, Protocol for the fast chromatin immunoprecipitation (ChIP) method. *Nat. Protoc.* **1**, 179–185 (2006).
57. J. Han, Q. Li, L. McCullough, C. Kettelkamp, T. Formosa, Z. Zhang, Ubiquitylation of FACT by the cullin-E3 ligase Rtt101 connects FACT to DNA replication. *Genes Dev.* **24**, 1485–1490 (2010).
58. A. E. Dodson, J. Rine, Heritable capture of heterochromatin dynamics in *Saccharomyces cerevisiae*. *eLife* **4**, e05007 (2015).
59. S. Devbhandari, J. Jiang, C. Kumar, I. Whitehouse, D. Remus, Chromatin constrains the initiation and elongation of DNA replication. *Mol. Cell* **65**, 131–141 (2017).
60. A. V. Makarova, J. L. Stodola, P. M. Burgers, A four-subunit DNA polymerase ζ complex containing Pol δ accessory subunits is essential for PCNA-mediated mutagenesis. *Nucleic Acids Res.* **40**, 11618–11626 (2012).
61. M. Marcel, Cutadapt removes adapter sequences from high-throughput sequencing reads. *EMBnet journal* **17**, 10–12 (2011).
62. B. Langmead, S. L. Salzberg, Fast gapped-read alignment with Bowtie 2. *Nat. Methods* **9**, 357–359 (2012).
63. A. Tarasov, A. J. Vilella, E. Cuppen, I. J. Nijman, P. Prins, Sambamba: Fast processing of NGS alignment formats. *Bioinformatics* **31**, 2032–2034 (2015).
64. F. Ramirez, D. P. Ryan, B. Gruning, V. Bhardwaj, F. Kilpert, A. S. Richter, S. Heyne, F. Dundar, T. Manke, deepTools2: A next generation web server for deep-sequencing data analysis. *Nucleic Acids Res.* **44**, W160–W165 (2016).
65. K. Brogaard, L. Xi, J. P. Wang, J. Widom, A map of nucleosome positions in yeast at base-pair resolution. *Nature* **486**, 496–501 (2012).
66. O. Flores, O. Deniz, M. Soler-Lopez, M. Orozco, Fuzziness and noise in nucleosomal architecture. *Nucleic Acids Res.* **42**, 4934–4946 (2014).

Acknowledgments: We thank D. Remus for the yeast strain and protocols for the purification of Pol δ and P. Burgers for antibodies against Pol32. **Funding:** This work was supported by National Institutes of Health grants R35GM118015 (Z.Z.), K99GM134180 (A.S.-C.), and R01HD093783 (F.C.) and UNH grants CIBBR P20-GM113131 (supporting the Mass Spectrometry Core facility at UNH) and R35GM126910 (S.J.). **Author contributions:** Conceptualization: A.S.-C. and Z.Z. Data analysis: X.H. and S.W.M. Investigation: A.S.-C., H.Z., and T. T. Visualization: A.S.-C. and X.H. Writing—original draft: A.S.-C. and Z.Z. Writing: A.S.-C., X.H., and Z.Z. Editing: All authors read and edit the text. Supervision: Z.Z., S.J., and F.C. **Competing interests:** The authors declare that they have no competing interests. **Data and materials availability:** All data needed to evaluate the conclusions in the paper are present in the paper and/or the Supplementary Materials. Raw and processed sequencing data generated in the course of this study can be accessed via the GEO database with accession number GSE203465. Requests for yeast strains and plasmids generated in this study should email Z.Z. email: (zz2401@cumc.columbia.edu) at Columbia University Irving Medical Center. A complete material transfer agreement may be needed.

Submitted 14 December 2023

Accepted 1 May 2024

Published 5 June 2024

10.1126/sciadv.adn5175